Vision Research 161 (2019) 1–11

Contents lists available at ScienceDirect

Vision Research

journal homepage: www.elsevier.com/locate/visres

Nonlinearities in the flicker electroretinogram: A tool for studying retinal dysfunction applied to early-stage diabetic retinopathy

J. Jason McAnany[a,b,*], Yi-Fan Chen[c], Karen Liu[a], Jason C. Park[a]

[a] Department of Ophthalmology and Visual Sciences, University of Illinois at Chicago, 1855 W. Taylor St., Chicago, IL 60612, USA
[b] Department of Bioengineering, University of Illinois at Chicago, 851 South Morgan St., Chicago, IL 60607, USA
[c] Center for Clinical and Translational Sciences, University of Illinois at Chicago, 914 S Wood Street, Chicago, IL 60612, USA

ARTICLE INFO

Keywords:
Electroretinogram
Subharmonic
Harmonic
Diabetic retinopathy

ABSTRACT

The flicker electroretinogram (ERG) is typically analyzed in terms of peak-to-trough amplitude and implicit time. However, additional important information may be captured by spectral-domain analysis of the ERG harmonics (responses that occur at multiples of the stimulus frequency). This study describes an approach to analyze the harmonic components of the flicker ERG and its application to patients who have early-stage non-proliferative diabetic retinopathy (NPDR). Of particular interest were the sub-harmonic components occurring at 1.5x and 2.5x the stimulus frequency that produce cycle-to-cycle variation in amplitude termed "period doubling." Twenty visually-normal subjects, 20 diabetic subjects who have no clinically-apparent retinopathy (NDR), and 20 diabetic subjects who have mild NPDR participated. ERGs were recorded in response to sinusoidal flicker (27–63 Hz) and Fourier analysis was performed to extract fundamental and harmonic response amplitudes. Linear quantile mixed models (LQMMs) were used to compare the amplitude of the response components among the three subject groups. Results indicated that the maximum sub-harmonic amplitude occurred in the stimulus frequency range of 33–38 Hz for all subjects. The LQMMs showed a significant sub-harmonic amplitude reduction for the mild NPDR subjects compared to the controls; sub-harmonic amplitude for the NDR subjects did not differ significantly from the controls. In contrast, the fundamental response did not differ among the groups for stimulus frequencies between 33 and 38 Hz. Modeling these results indicated that subharmonic amplitude loss in mild NPDR subjects may be attributed to attenuated feedback occurring early in the retina, possibly at the synapse of cone photoreceptors and OFF bipolar cells.

1. Introduction

The flicker electroretinogram (ERG) is a common measure of cone pathway function that has been used to study the normal visual system and that of patients who have inherited and acquired retinal dysfunction. The International Society for Clinical Electrophysiology of Vision (ISCEV) recommends recording the flicker ERG in response to a periodic train of pulses presented at approximately 30 Hz (McCulloch et al., 2015). The flicker response is typically analyzed by measuring the peak-to-trough amplitude and the implicit time (i.e. time from stimulus to response peak). Although the flicker ERG recorded and analyzed according to conventional standards is a sensitive and useful measure of cone pathway function, additional valuable information may be contained in the response that is not apparent from standard peak-to-trough amplitude and implicit time measurements made in the time-domain.

To extract additional information, Fourier analysis has been applied as an alternative approach to analyze the human flicker ERG in both basic and clinical research studies (e.g., Alexander, Barnes, & Fishman, 2001; Hassan-Karimi et al., 2012; McAnany & Nolan, 2014; Sieving, Arnold, Jamison, Liepa, & Coats, 1998). An important advantage of Fourier analysis is that the amplitude and timing of the fundamental (F; the response component that occurs at the stimulus frequency) is obtained, in addition to other spectral components that are not readily quantified by standard time-domain measures (the "harmonics" that occur at multiples of the stimulus frequency). The nonlinear nature of the human flicker ERG has been studied for decades, primarily in visually-normal individuals (Baker & Hess, 1984; Burns, Elsner, & Kreitz, 1992; Gouras & Gunkel, 1962; Odom, Reits, Burgers, & Riemslag, 1992), but there are also reports of the effect of retinal disease on the

* Corresponding author at: University of Illinois at Chicago, Department of Ophthalmology and Visual Sciences, 1855 W. Taylor St., MC/648, Chicago, IL 60612, USA.
E-mail address: jmcana1@uic.edu (J.J. McAnany).

https://doi.org/10.1016/j.visres.2019.05.005
Received 23 January 2019; Received in revised form 7 May 2019; Accepted 12 May 2019
Available online 05 June 2019
0042-6989/

nonlinear components of the flicker ERG (Alexander, Fishman, & Grover, 2000; Gouras & Gunkel, 1964; Viswanathan, Frishman, & Robson, 2002). Importantly, there is evidence that the fundamental and harmonic components of the flicker ERG may be generated by different retinal cell populations (Porciatti & Falsini, 1993; Viswanathan et al., 2002). As such, comparison of the fundamental and harmonics may provide insight into the sites and mechanisms of retinal disease (e.g., Alexander et al., 2001; McAnany & Park, 2018b; Sieving et al., 1998; Viswanathan et al., 2002).

Studies in early-stage diabetic retinopathy provide an example of the potential value in comparing the fundamental and harmonics to better understand retinal dysfunction. That is, the fundamental and harmonic components of the flicker response elicited by slow flicker (16 Hz) were found to be normal in these individuals, but for higher temporal frequencies (e.g. 50–100 Hz), there was a significant loss of fundamental amplitude (McAnany & Park, 2018a, 2018b). Interestingly, the mean fundamental response elicited by 62.5 Hz flicker was reduced significantly for diabetic subjects who had mild or no retinopathy, but their fourth harmonic response to 16-Hz flicker (equivalent to 64 Hz) was not (McAnany & Park, 2018b). These findings can be explained within the context of a linear-nonlinear-linear cascade model of retinal processing that posits a retinal nonlinearity "sandwiched" between two linear filters (Alexander et al., 2000; Burns et al., 1992; Spekreijse & Reits, 1982). As discussed in detail elsewhere, changes in the properties of the first linear filter, which is thought to be localized to the photoreceptors, could attenuate the fundamental response at high temporal frequencies without affecting the high-frequency harmonics elicited by slow flicker (Alexander et al., 2000; McAnany & Park, 2018b). Thus, comparison of the fundamental and harmonics has suggested an early retinal site for the high-frequency flicker ERG reduction in diabetic retinopathy (McAnany & Park, 2018b).

In addition to the harmonics that occur at 2x and 3x the stimulus frequency (2F and 3F) that have been widely studied, response components can also occur at "subharmonics" (e.g. 0.5x, 1.5x and 2.5x the stimulus frequency; F/2, 3F/2, 5F/2). The subharmonic components result in an alternation in response amplitude and/or waveform shape from response cycle-to-cycle that has been termed "synchronous period doubling" (Crevier & Meister, 1998). Synchronous period doubling is thought to be due to a nonlinear feedback signal that decays exponentially and alters response gain (Crevier & Meister, 1998). In addition, electrical coupling across neural elements is needed to explain the synchronicity of the response. Crevier and Meister (1998), who provided the initial description of synchronous period doubling in the salamander retina, proposed that the phenomenon originates at the synapse between the cone photoreceptors and OFF bipolar cells. The subharmonics have not been reported in patient populations to date, but these components may be abnormal in early-stage diabetic retinopathy given that period doubling is also thought to originate at an early retinal site (Crevier & Meister, 1998).

The purpose of the present study was to examine the harmonic components of the flicker ERG in diabetic subjects who have no diabetic retinopathy (NDR) or mild nonproliferative diabetic retinopathy (NPDR). Our goal is to highlight the usefulness of analyzing nonlinearities in the flicker ERG as a means to better understand the sites and mechanisms of retinal disease. The flicker ERG was recorded across a broad range of temporal frequencies, and the fundamental, integer harmonics, and subharmonics were compared between the control and diabetic subject groups. The focus of the present study was largely on the subharmonic components of the flicker ERG, as these components have not been evaluated in patient populations. The results were examined in the context of the linear-nonlinear-linear cascade model described above, with the addition of a nonlinear feedback stage to account for period doubling.

2. Method

2.1. Subjects

The flicker ERG data that form the basis for the present report were obtained from a previous study of the flicker ERG in diabetes (McAnany & Park, 2019). The sample consisted of 40 individuals diagnosed with type-2 diabetes mellitus (DM) who were recruited from the Department of Ophthalmology and Visual Sciences at the University of Illinois at Chicago (13 male and 27 female; mean age ± SD: 52.8 ± 8.3 years). In addition, 20 visually-normal, non-diabetic control subjects were also recruited (8 male and 12 female; mean age ± SD: 51.9 ± 12.2 years). The subject characteristics are detailed in the original report (McAnany & Park, 2019). In brief, each subject was examined by a retina specialist and the subjects were clinically classified as diabetic with no clinically-apparent DR (N = 20) or diabetic with mild NPDR (N = 20) according to the early treatment of diabetic retinopathy study (ETDRS) scale (Davis et al., 1998). Other than diabetes, no subject had systemic disease known to affect retinal function, other ocular disease, or significant cataract. No subject had a history of panretinal photocoagulation, but three mild NPDR subjects had received anti-VEGF injections and had diabetic macular edema at the time of testing.

The control subjects had best-corrected Sellen visual acuity of approximately 20/20 or better, as assessed with the Lighthouse distance visual acuity chart, and normal letter contrast sensitivity as measured with a Pelli-Robson chart. There was no significant difference in mean age between the control and DM subjects ($F = 0.21$, $p = 0.81$). Measurements from all control subjects were obtained from the right eye, with the left eye patched. For the DM subjects, the stage of NPDR was the same for the two eyes, with the exception of two subjects who had asymmetric disease (mild NPDR in one eye and NDR in the other); for these two subjects, the NDR eye was tested and the fellow eye was patched. The studies conformed to the tenants of the Declaration of Helsinki, institutional review board approval was obtained at the University of Illinois at Chicago, and the experiments were undertaken with the understanding and written consent of each subject.

2.2. Apparatus, stimuli, procedure, and analysis

Sinusoidal flicker stimuli were generated by and presented in a ColorDome desktop ganzfeld system (Diagnosys LLC, Lowell, MA) that we have used previously and described elsewhere (McAnany & Park, 2019; Park, Cao, Collison, Fishman, & McAnany, 2015). The subject was first light adapted for 2 min to a uniform field that was composed of 3.7 log Td of middle-wavelength light (516-nm peak) and 3.7 log Td long-wavelength light (632-nm peak), assuming a dilated pupil diameter of 8 mm. The uniform field was modulated sinusoidally at temporal frequencies ranging from 6 Hz to 100 Hz in steps of approximately 0.06 log units. However, only the frequency range of 27.8 Hz to 62.5 Hz will be considered in the present study, because responses to lower and higher stimulus frequencies generally lack period doubling (Alexander & Raghuram, 2007; Alexander, Levine, & Super, 2005; Alexander, Raghuram, & McAnany, 2008). The Michelson contrast of the sinusoidal modulation was 100%. Each flicker train had a duration of approximately 1 s, with the exact duration depending on the stimulus period. A minimum of 5 responses for each temporal frequency were obtained and averaged for analysis. Between presentations of the flicker stimulus, the ganzfeld was illuminated uniformly by the steady adapting field.

The pupil of the tested eye was dilated with 2.5% phenylephrine hydrochloride and 1% tropicamide drops. ERGs were recorded with DTL electrodes, and gold-cup electrodes were used as reference (ear) and ground (forehead). Amplifier bandpass settings were 0.30 to 500 Hz and the sampling frequency was 2 kHz. The initial and final few cycles of the flicker waveforms were omitted, as these cycles can contain onset and offset transients. The remaining steady-state response

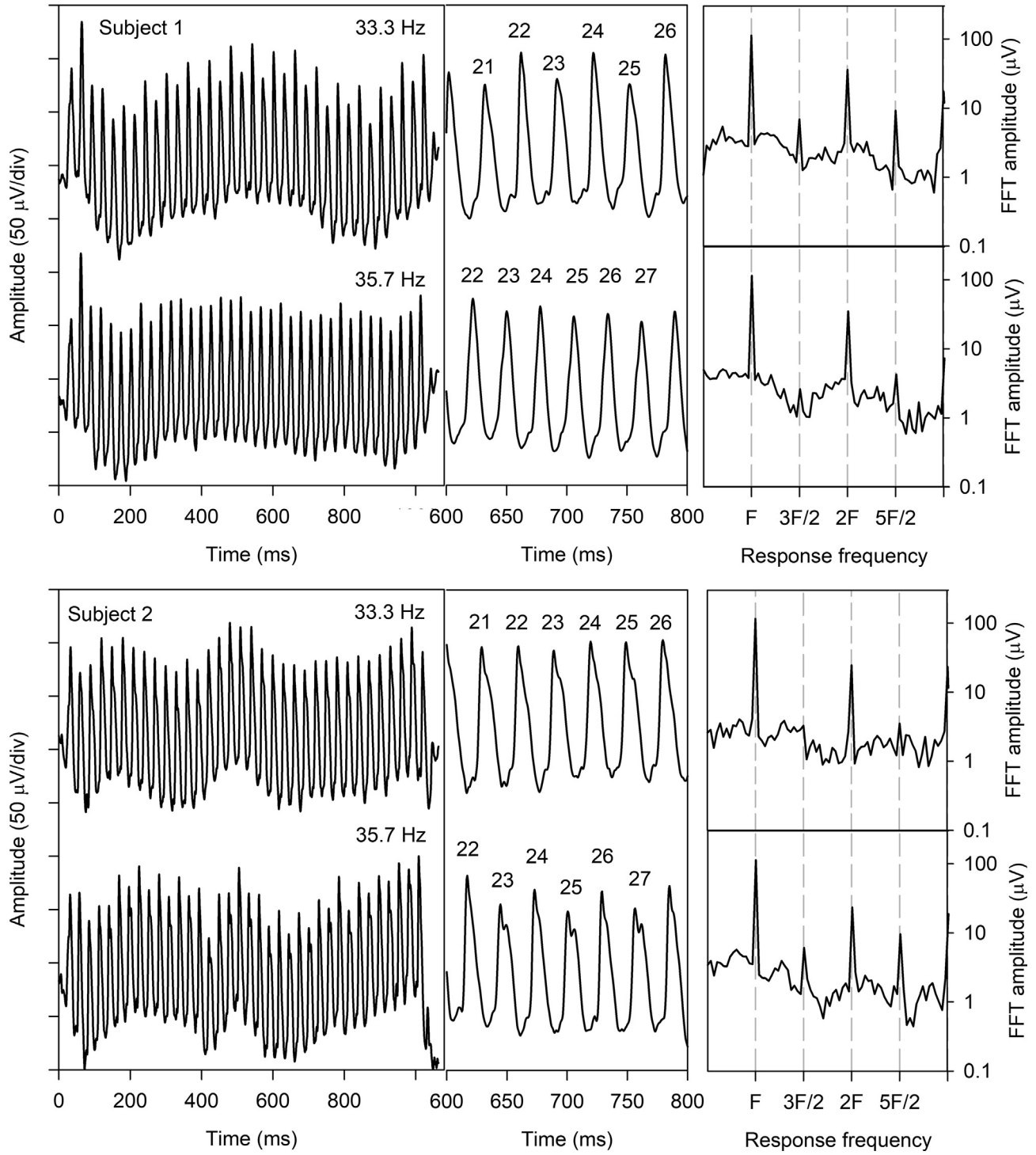

Fig. 1. Illustration of period doubling in the flicker ERG of Subject 1 (upper panels) and Subject 2 (lower panels) obtained at stimulus frequencies of 33.3 Hz (top traces) and 35.7 Hz (bottom traces). The middle panels show expanded views of 6 response cycles recorded near the middle of the flicker trains. The right panels show the Fourier spectra for the waveforms, with the fundamental (F), second harmonic (2F), and subharmonics (3F/2 and 5F/2) marked by vertical dashed lines.

was processed using Fourier analysis to derive the amplitude of the fundamental and harmonics of the flicker ERG.

3. Results

3.1. Example of synchronous period doubling

Fig. 1 illustrates the phenomenon of synchronous period doubling for two control subjects. For Subject 1, there was an obvious alternation in amplitude from cycle-to-cycle at 33.3 Hz (top trace), with larger amplitude for the even cycles compared to the odd cycles; the middle panel shows an expanded time-base for easier inspection of the waveform shape. The right panel shows the Fourier spectrum derived from the waveform. There was a large fundamental component, as expected, as well as components at 2F and 3F (not shown). In addition, peaks in the spectrum are apparent at 3F/2 and 5F/2. These subharmonic peaks are generated by the cycle-to-cycle alternation in waveform amplitude/shape (i.e. period doubling). At the slightly higher stimulus temporal

frequency of 35.7 Hz, the cyclic variation in amplitude was less apparent for Subject 1 (upper panel, lower trace). The Fourier spectrum at this stimulus frequency has little amplitude at 3F/2 and 5F/2, which is consistent with the generally uniform appearance of the cycles in the waveform. The lower panels show the waveforms obtained at 33.3 Hz and 35.7 Hz for Subject 2. For this subject, cyclic variation in amplitude was not apparent at 33.3 Hz, but it was apparent at 35.7 Hz. In addition to the cycle-to-cycle variation in amplitude at 35.7 Hz, there was also variation in the shape of the response, with the odd cycles exhibiting a bifurcated peak. The Fourier spectra show little subharmonic response amplitude at 33.3 Hz, but obvious subharmonic peaks at 35.7 Hz for this subject, as expected from the shapes of the waveforms. These examples highlight three previously reported features of period doubling (Alexander & Raghuram, 2007; Alexander et al., 2005, 2008): 1) period doubling occurs over a narrow band of stimulus frequencies; 2) there are inter-subject differences in the stimulus frequencies at which the phenomenon occurs; 3) period doubling can be characterized as cycle-to-cycle variation in amplitude and/or waveform shape. In addition, previous work has also shown that when the stimulus is repeated, the response alternation begins on the same cycle from trial to trial (Alexander et al., 2008). This consistency in the phenomenon was shown for all temporal frequencies and for all subjects tested (Alexander et al., 2008). Given the within-subject consistency in the onset of period doubling, the analyses described below were based on the mean of at least five ERG responses obtained at each stimulus temporal frequency.

3.2. Synchronous period doubling across temporal frequency

The mean fundamental and harmonic response components at each stimulus temporal frequency were derived by Fourier analysis. As noted above, an important advantage of Fourier analysis is that the harmonic components can be extracted, which provides a means to quantify waveform shape. That is, given the sinusoidal stimulus, the ERG is also expected to be sinusoidal, if the retina responds linearly. Harmonic distortion in the shape of the response must arise from nonlinearities in the retina and the harmonic components can be used to quantify the shape of the response. Fig. 2 plots mean log ERG amplitude for the fundamental, F/2 subharmonic, and harmonics of the subharmonic (3F/2, 5F/2) across a range of stimulus temporal frequencies. Data are shown for the control subjects (black circles), NDR subjects (green squares), and mild NPDR subjects (red triangles). There was a strong response component at the stimulus frequency (F), as expected (upper left panel). For moderate stimulus temporal frequencies (27.8–38.5 Hz) there were small amplitude differences among the three subject groups. For higher stimulus frequencies (41.7–62.5 Hz), larger differences in amplitude emerged among the three groups, as shown previously (McAnany & Park, 2018b).

The mean amplitude of the subharmonic (F/2) for each subject group is shown in the upper right panel. The amplitude of the F/2 noise across stimulus temporal frequency is represented by the gray range. The noise amplitude was defined as the mean of the amplitudes measured at frequencies that neighbor the response frequency of interest. For example, for the 33.3 Hz stimulus, the F/2 response (16.6 Hz) noise was taken as the mean amplitude measured at 15.5 Hz and 17.7 Hz. The F/2 component generally did not exceed the noise level, with the exception of responses measured at the highest temporal frequencies. As such, the F/2 data will not be considered further.

The mean amplitude of the harmonics of the subharmonic (3F/2 and 5F/2) are shown in the bottom row for each subject group. At the lower range of stimulus frequency (27.8–31.3 Hz), the responses were small and generally did not exceed the noise. In contrast, for moderate stimulus frequencies (33.3–38.5 Hz), substantial response amplitudes were observed that exceeded the noise, with a maximum at 35.7 Hz for all subject groups. The 3F/2 and 5F/2 amplitude decreased at higher stimulus frequencies (41.7–62.5 Hz). Thus, period doubling, as quantified by the 3F/2 and 5F/2 components, was tuned to a relatively narrow band of stimulus frequencies for each subject group, peaking at 35.7 Hz. These data are consistent with previous work, which also showed maximum period doubling at a stimulus frequency near 35 Hz in visually-normal subjects (Alexander et al., 2008).

3.3. Amplitude analyses for individual subjects for each response component

The data of Fig. 2 show the combined responses for subjects within each group, but it is of interest to examine the responses of individual subjects, because there are inter-subject differences in the magnitude of period doubling and the stimulus frequency band over which it occurs (e.g. Fig. 1). Fig. 3 shows log amplitude for each subject (controls, black circles; NDR subjects, green squares; mild NPDR subjects, red triangles); the group medians are indicated by the horizontal lines. Fundamental response amplitudes are shown in the top row, whereas the 3F/2 and 5F/2 amplitudes are shown in the middle and lower panels, respectively. Only the three frequencies at which the maximum period doubling occurred are shown (33.3 Hz left column, 35.7 Hz middle column, 38.5 Hz right column). In this figure, the noise, as defined above, was subtracted from the response. Non-detectable responses in which the noise was equal to or larger than the response are indicated by “ND.”

The F amplitude was similar for the three subject groups for the three stimulus frequencies shown. In contrast, differences among the three groups were apparent for the 3F/2 and 5F/2 amplitudes. There was a small reduction in the 3F/2 amplitude for the NDR subjects compared to the controls at 33.3 Hz and 35.7 Hz. Losses of 3F/2 amplitude were more apparent for the mild NPDR group at each stimulus frequency. In fact, most of the mild NPDR subjects did not have a detectable 3F/2 response at 33.3 Hz (the horizontal bar that marks the median falls in the ND range). Likewise, there were only small differences in 5F/2 amplitude for the NDR subjects compared to the controls (bottom row). For the mild NPDR subjects, loss of 5F/2 amplitude was apparent, and most of the mild NPDR subjects had a non-detectable 5F/2 response at 33.3 Hz.

The integer harmonics of the fundamental (2F and 3F) were evaluated to determine whether the amplitude loss is specific to the subharmonics or represents a more general abnormality in the harmonic response components. Fig. 4 shows the noise-corrected log amplitude for 2F (top row) and 3F (bottom row) for the three subject groups. As in Fig. 3, only the three stimulus frequencies at which the maximum period doubling occurred are shown (33.3 Hz left column, 35.7 Hz middle column, 38.5 Hz right column). The 2F log amplitude was similar for the three subject groups for the three temporal frequencies examined. The amplitude of the 3F component was slightly reduced for the NDR and mild NPDR subjects compared to the controls (average of 0.12 and 0.22 log units for the NDR and mild NPDR groups averaged over the three frequencies).

The data shown in Figs. 3 and 4 were analyzed quantitatively using linear quantile mixed models that were programmed in R (version 3.4.1 with the lqmm package), given the non-normal distribution of the amplitude data (Geraci & Bottai, 2007, 2014; Geraci, 2014). In each model, group (control, NDR, mild NPDR), stimulus frequency (33.3 Hz, 35.7 Hz, 38.5 Hz), and their interactions were included as main predictors; a random intercept was added at the subject level to account for subject dependence (i.e. repeated measures on the same subject). A separate model was constructed to assess the group differences (NDR vs control; mild NPDR vs control) in median amplitude for each of the five frequency components (F, 2F, 3F, 3F/2, 5F/2). Values in which the noise was equal to or larger than the response were excluded from the analysis, as the response amplitude cannot be defined for these measurements. The results of the analysis indicated that there were no significant differences in F amplitude for the patient groups compared to the control (NDR coefficient of 0.05, $p = 0.78$; mild NPDR coefficient of -0.17, $p = 0.29$). For the 3F/2 component, there was a significant

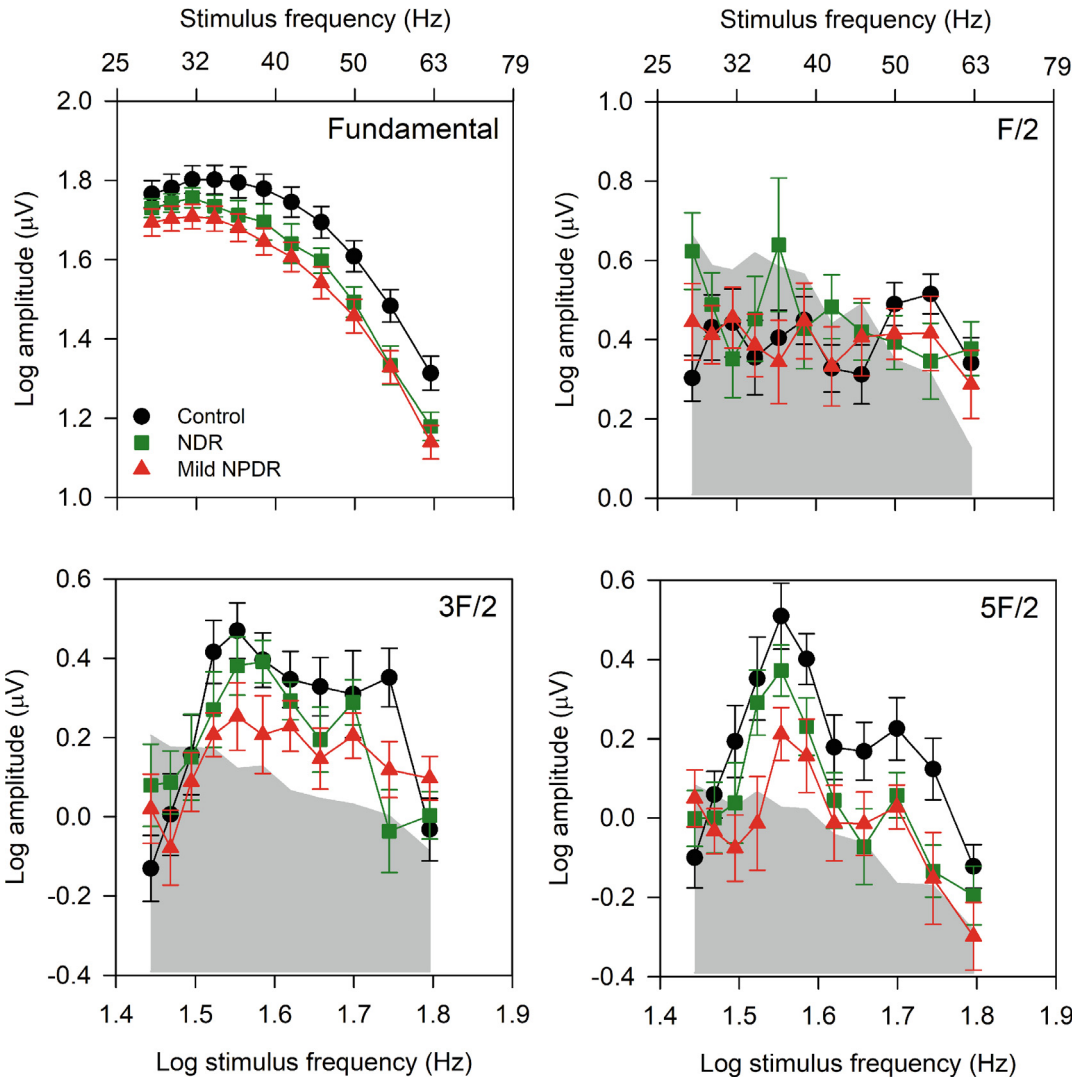

Fig. 2. Mean log amplitude (± SEM) is plotted as a function of log stimulus temporal frequency for the response fundamental (upper left), F/2 component (upper right), 3F/2 component (lower left), and 5F/2 component (lower right). Linear equivalents of the log stimulus frequency values are shown along the top x-axes. Data are shown for the controls (black circles), NDR subjects (green squares), and mild NPDR subjects (red triangles). The gray regions represent the noise levels, as described in the text.

amplitude loss for the mild NPDR group (coefficient of −0.81, p = 0.01), but not the NDR group (coefficient of −0.04, p = 0.89). Likewise, for the 5F/2 component, there was a significant amplitude loss for the mild NPDR group (coefficient of −0.94, p = 0.01), but not the NDR group (coefficient of −0.48, p = 0.09). There were no significant differences in 2F amplitude for the patient groups compared to the control group (NDR coefficient of −0.30, p = 0.06; mild NPDR coefficient of −0.13, p = 0.36), but there were borderline-significant amplitude losses in 3F for both patient groups (NDR group coefficient of −0.26, p = 0.04; mild NPDR group coefficient of −0.42, p = 0.05). In summary, the median subharmonic amplitudes (3F/2 and 5F/2) were markedly reduced for the mild NPDR group (reductions of 0.81 to 0.94 log units), whereas the integer harmonic amplitudes were less affected (0.13 to 0.42 log unit reduction in 2F and 3F, respectively).

3.4. Receiver operating characteristic analysis

Receiver operating characteristic (ROC) curves were constructed as an additional approach to compare the subharmonic amplitudes among the subject groups. Fig. 5 plots sensitivity (fraction of diabetic subjects classified as abnormal) as a function of 1-specificity (fraction of control subjects classified as abnormal) for the three stimulus temporal frequencies shown in Figs. 3 and 4. Results for the NDR and mild NPDR subjects are shown in green and red, respectively. The area under the curve (AUC) and associated p-value are provided in each panel for both diabetic groups. The fundamental (top row) was capable of separating the mild NPDR group from the controls at 38.5 Hz (AUC = 0.70, p = 0.03); the AUC was borderline non-significant for the 33.3 Hz and 35.7 Hz stimulus frequencies for these subjects. The fundamental did not provide a statistically significant separation for the NDR subjects at any stimulus frequency. In contrast, the AUC values were statistically significantly for the subharmonics (both 3F/2 and 5F/2) at all stimulus frequencies for the mild NPDR subjects. The AUC value was statistically significant only for the 5F/2 subharmonic at 38.5 Hz for the NDR subjects. For the 38.5 Hz 5F/2 component, the optimal cutoff was approximately 1.1 μV for both the NDR and mild NPDR subjects. For this cutoff, the sensitivity and specificity were 0.65 for the NDR group, whereas for the mild NPDR group, the sensitivity and specificity were 0.85 and 0.65, respectively. Thus, the 5F/2 subharmonic elicited by 38.5 Hz flicker may have the greatest clinical utility of the subharmonics examined, but this finding should be confirmed in a larger sample of diabetic subjects.

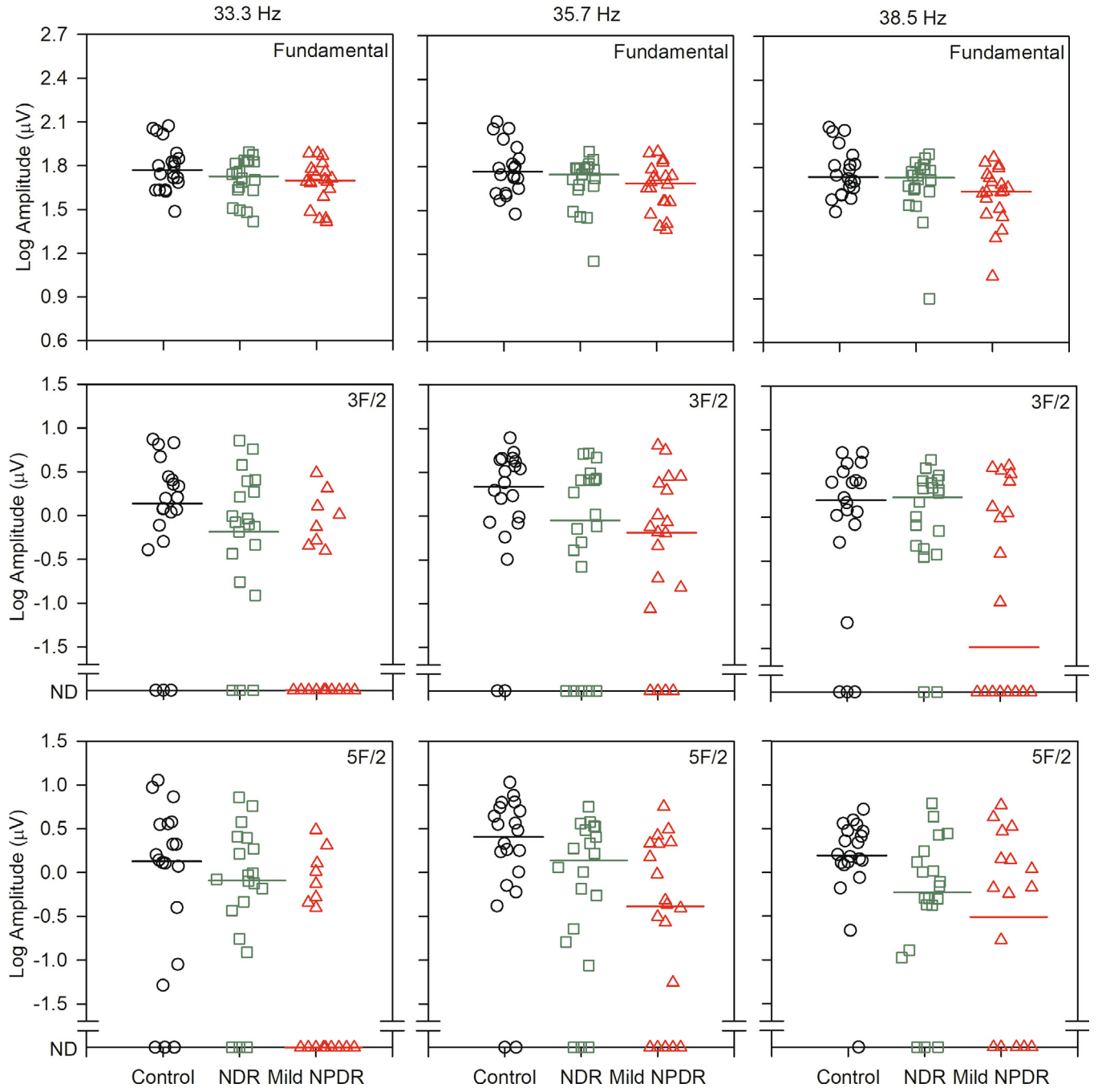

Fig. 3. Noise-corrected log amplitude is shown for the controls (black circles), NDR subjects (green squares), and mild NPDR subjects (red triangles). The fundamental response for each subject is shown in the top row, whereas the 3F/2 and 5F/2 harmonics are shown in the middle and lower rows, respectively. Data are presented for the three stimulus temporal frequencies that elicited the maximum period doubling (33.3 Hz, left column; 35.7 Hz, middle column; 38.5 Hz, right column). The horizontal bars mark the median of each group and "ND" indicates responses that were not detectable, as described in the text.

3.5. Quantitative model of synchronous period doubling in diabetes

Crevier and Meister (1998) proposed a quantitative model of synchronous period doubling based on data recorded from salamander retina. This model was subsequently used to account for period doubling in the human flicker ERG (Alexander et al., 2005). According to the model, period doubling can be explained by non-linear feedback that alters response gain. Specifically, the flicker ERG response (R) to a repetitive flicker train of contrast (C) is determined by response gain (g), which depends on a variable feedback (y):

$$R = C \cdot g(y). \tag{1}$$

In their formulation, Crevier and Meister (1998) proposed that:

$$g(y) = 1/(1 + y^4). \tag{2}$$

For a repetitive flicker train with a temporal frequency (f), the response to the i^{th} stimulus cycle is:

$$R_i = C \cdot g(y_i), \tag{3}$$

where

$$y_i = e^{-1/f\tau}[BC \cdot g(y_{i-1}) + y_{i-1}]. \tag{4}$$

In Eq. (4), B is a scaling factor that controls the magnitude of the feedback signal (y), and τ is the time constant of the feedback decay.

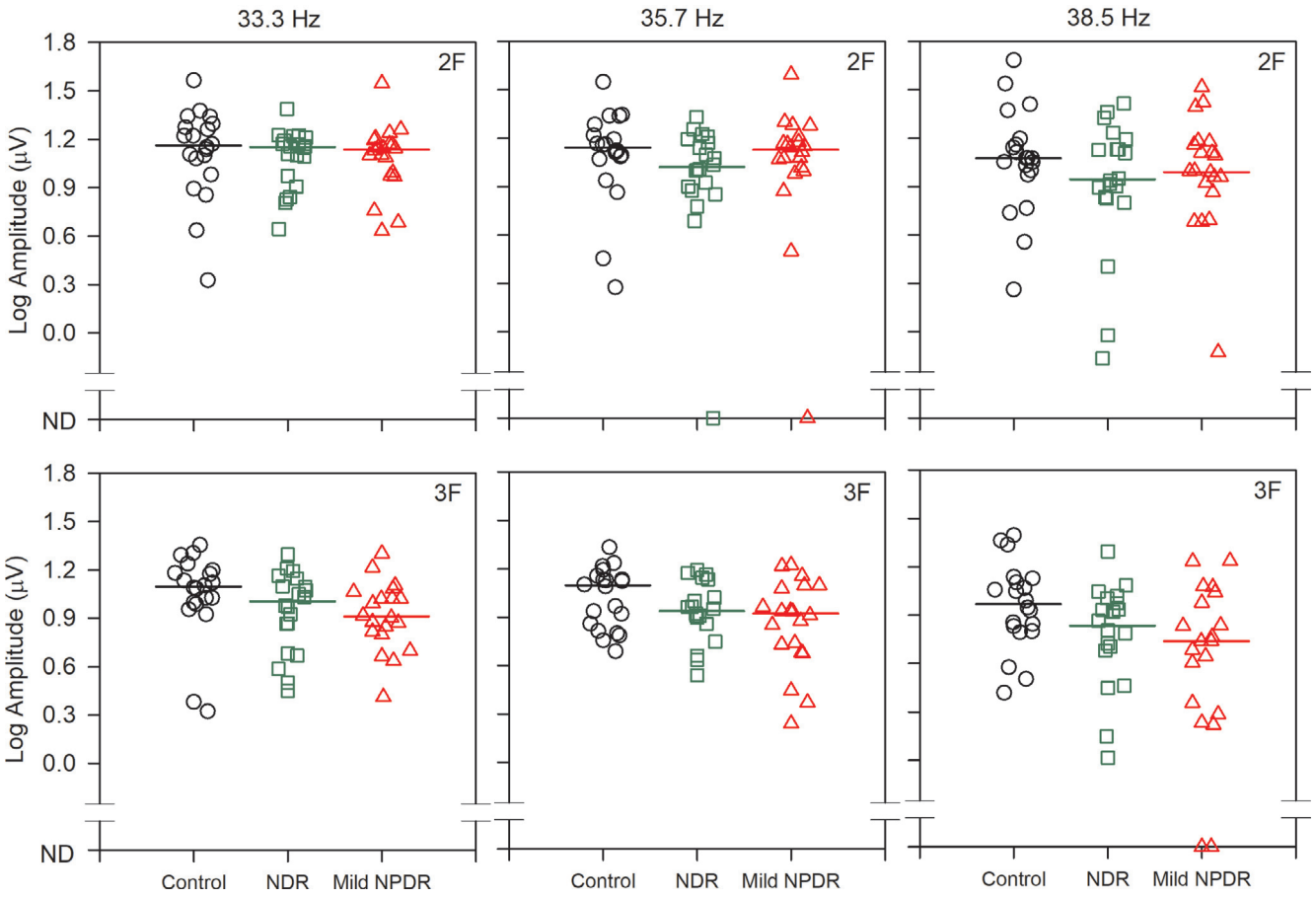

Fig. 4. Noise-corrected log amplitude is shown for the 2F (top row) and 3F (bottom row) response components. All other conventions are as in Fig. 3.

Consequently, in this model, B and τ govern the properties of synchronous period doubling. A decrease in B reduces the magnitude of the amplitude alternation (and shape alternation) from cycle-to-cycle, whereas a change in τ shifts the stimulus frequency band over which period doubling occurs. Conceptually, a large response on a given cycle (R_i) generates strong feedback (y_i) that reduces the response to the subsequent stimulus cycle (R_{i+1}). The reduced response (R_{i+1}), in turn, generates weaker feedback (y_{i+1}) that increases the response and feedback for the next stimulus cycle. Thus, a varying gain produces a systematic alteration in response amplitude from cycle-to-cycle.

The effect of manipulating the parameters B and τ is shown in Fig. 6 (left). These "bifurcation plots" were generated using the nonlinear feedback model of Crevier and Meister defined above (also discussed in detail in Crevier and Meister [1998] and Alexander et al. [2005]). In Fig. 6 (left), relative ERG response amplitude is plotted as a function of log stimulus temporal frequency. For the control subjects (black), the ERG amplitude can take one of two different values over the frequency range of approximately 30–40 Hz. For example, the even cycles can have larger amplitude than the odd cycles, as shown in Fig. 1. If the value of B is reduced in the DM subjects (model example in red; upper left panel), the magnitude of period doubling would decrease, and the cycle-to-cycle amplitude would have little variation. In this example, B was reduced from 3.98 to 3.90. Alternatively, if the value of τ is increased in the DM subjects (model example in red; lower left panel), the magnitude of period doubling would be like that of the controls, but the frequency range over which the phenomenon occurs would shift to lower stimulus temporal frequencies. In this example, τ was increased from 30 ms to 38 ms.

Example data from three subjects are shown in the right column of Fig. 6, which permits comparisons to the predicted effects of changing B and τ. Peak-to-trough amplitudes are shown for 14 cycles that were recorded near the middle of the flicker across a range of stimulus temporal frequencies for a control subject and two NDR subjects. Amplitudes for the even cycles are shown in blue and the odd cycles are shown in gray. The solid lines represent the mean amplitude for even (blue) and odd (gray) cycles at each temporal frequency. For the control subject, the amplitude at 35.7 Hz (marked by the vertical dashed line) took one of two values, with the amplitude of the even cycles being approximately 1.4x larger than that of the odd cycles. For this control subject, the cycle-to-cycle amplitude alternation was sharply tuned to 35.7 Hz (note that other manifestations of period doubling such as cycle-to-cycle variation in waveform shape are not well captured by this plot). The seven amplitude values for the even cycles tended to overlap, with relatively little variation. Clustering of the amplitude values for the odd cycles was also observed. Likewise, for NDR subject number 1 (NDR1), the amplitude of the even cycles was larger than that of the odd cycles at 35.7 Hz. There were also amplitude differences between the even and odd cycles at the neighboring stimulus frequencies (33.3 Hz and 38.5 Hz) for this NDR subject. The seven amplitude values for the even cycles varied (the same was found for the odd cycles), which is in contrast to the minimal variation within even and odd cycles observed for the control. Nevertheless, NDR1 provides an example of a diabetic subject whose flicker ERG waveform exhibited period doubling. The stimulus temporal frequency range over which period doubling occurred was similar to that of the control, but the magnitude of the phenomenon was somewhat attenuated. An example of an NDR subject who generally lacked period doubling is also shown (NDR2). Careful inspection shows that the odd cycles tended to be slightly larger, on average, at 38.5 Hz for this subject, but the cycle-to-cycle amplitude differences were small. Taken together, Fig. 6 indicates that

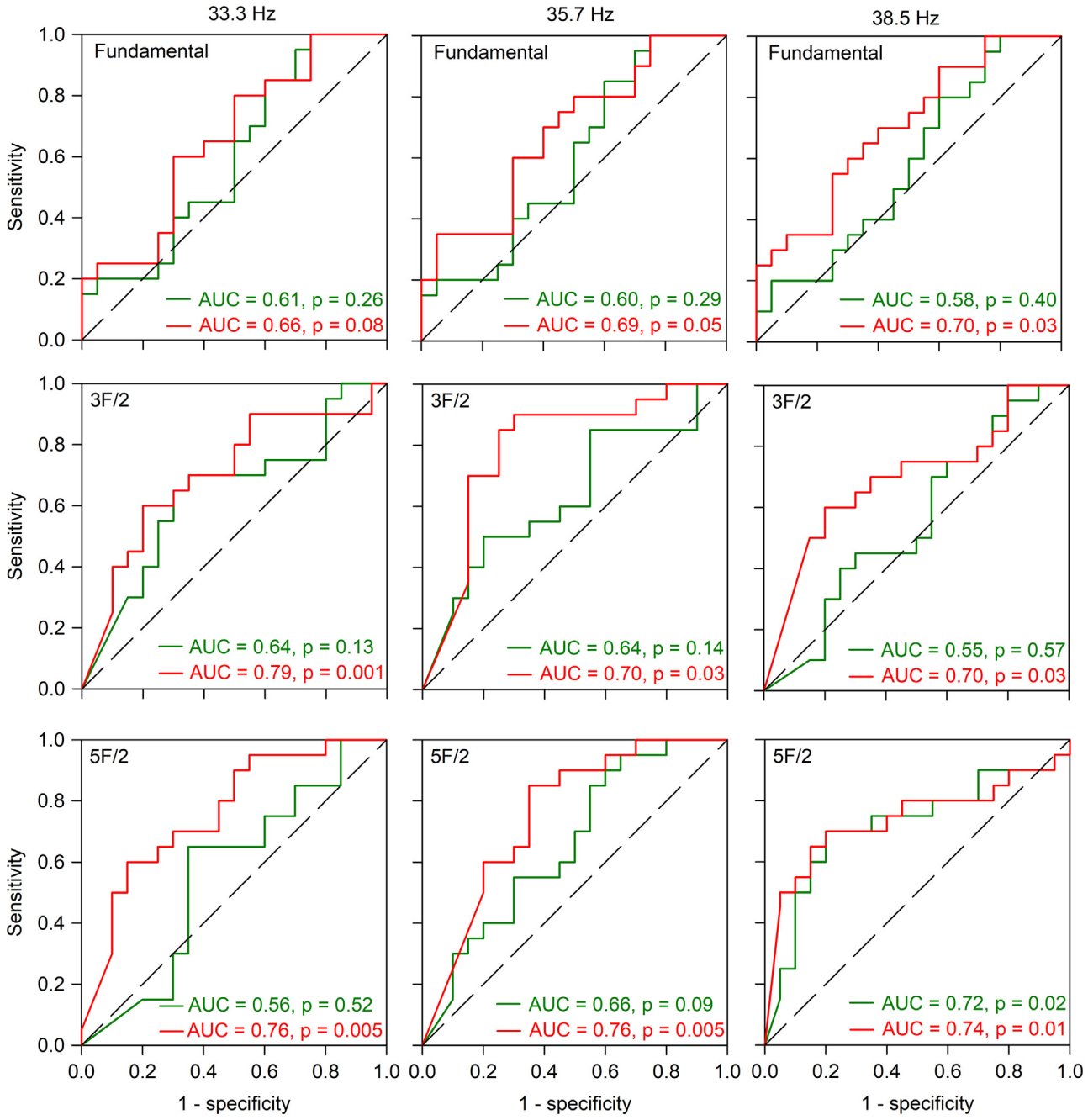

Fig. 5. Receiver operating characteristic curves for the NDR (green) and mild NPDR (red) subjects. The fraction of the diabetic subjects classified as abnormal (sensitivity) is plotted as a function of the fraction of control subjects classified as abnormal (1-specificity; false positives). Data for three stimulus frequencies are shown (33.33 Hz, left column), (35.7 Hz, middle column), and (38.5 Hz, right column). Curves for the fundamental (top row), 3F/2 (middle row), and 5F/2 (bottom row) are shown. Each panel lists the AUC and associated p-value.

the DM subject data are more consistent with reduced *B* than increased τ. That is, period doubling tends to be attenuated in the DM subjects, not shifted to lower (or higher) temporal frequencies. This can also be seen in the group average data of Fig. 2, which shows that the transfer functions for the 3F/2 and 5F/2 components had the same shape for the controls and DM subjects (e.g. similar bandwidth and peak at 35.7 Hz); it is only the amplitude of these components that was reduced in the DM subjects.

4. Discussion

This study examined the fundamental and harmonic response components of the flicker ERG in diabetic subjects who have mild or no NPDR. Although previous work has examined non-linearities in the flicker response (Alexander et al., 2000; Baker & Hess, 1984; Burns et al., 1992; Gouras & Gunkel, 1962; Odom et al., 1992; Viswanathan et al., 2002), we sought to highlight the use of these as a tool for better understanding the site of disease action. The focus of the present study was primarily on the subharmonic components of the flicker ERG, as these are markers of synchronous period doubling and have not been evaluated in any patient population to date. The primary finding was a loss of subharmonic amplitude (at response frequencies corresponding to 3F/2 and 5F/2) in subjects who had mild NPDR. This finding indicates reduced or absent period doubling in these individuals. In

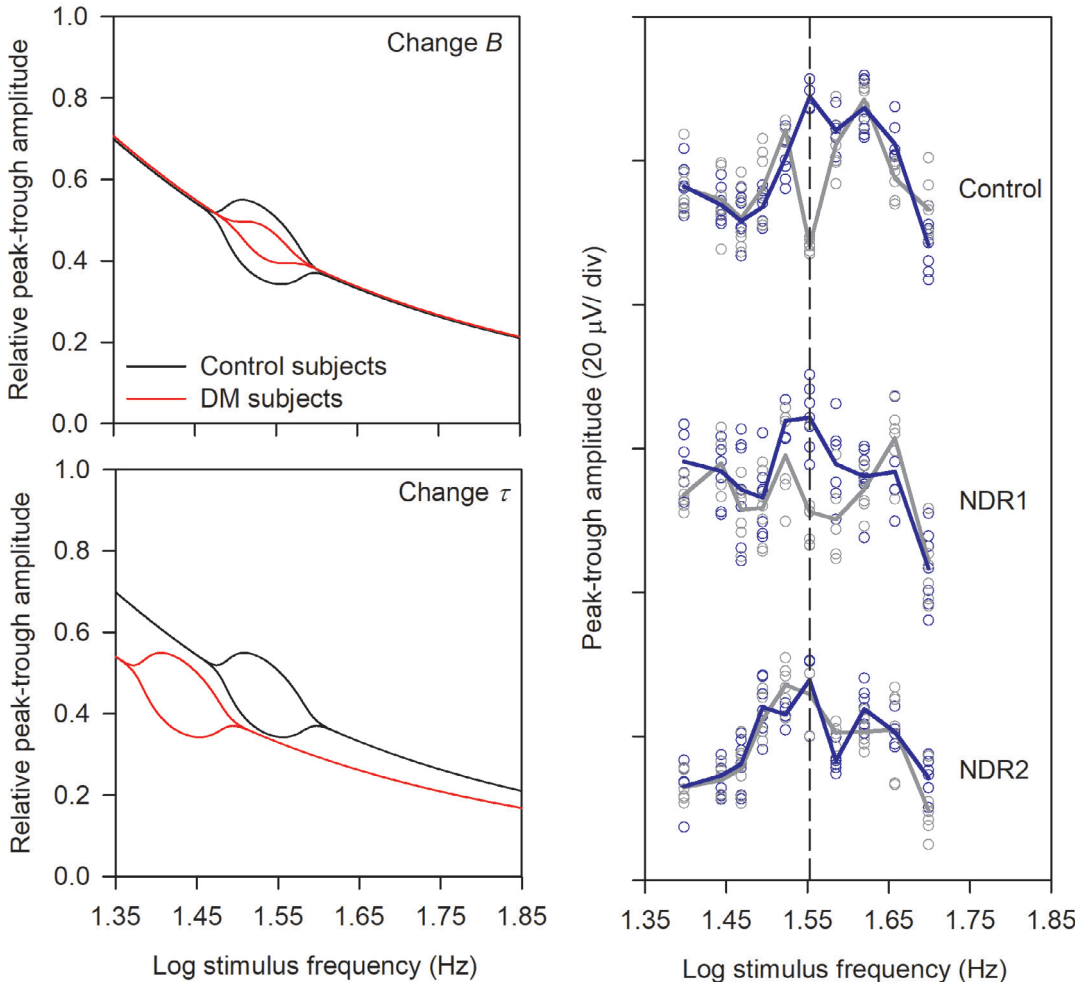

Fig. 6. Model of the temporal transfer function for the controls (black) and diabetic subjects (red) that describe the effects of changing the model parameters on period doubling (left panels). Relative response amplitude is plotted as a function of log stimulus temporal frequency. The left panels illustrate the predicted effects of reducing the parameter *B* (top) and increasing parameter τ (bottom). Amplitude for 14 cycles recorded near the middle of the flicker train are shown for a representative control subject and two NDR subjects (right panel). Each circle represents the amplitude for a single cycle, with even cycles shown in blue and odd cycles shown in gray. The solid lines are the mean even (blue) and odd (gray) cycle amplitudes for each stimulus temporal frequency. The vertical dashed line marks the stimulus temporal frequency of 35.7 Hz, which is the frequency at which the maximum cycle-to-cycle amplitude variation occurred. (For interpretation of the references to colour in this figure legend, the reader is referred to the web version of this article.)

contrast, the fundamental and harmonic components corresponding to 2F and 3F were either not affected or were only minimally attenuated for frequencies at which the subharmonics were markedly attenuated.

Consistent with previous work (Alexander & Raghuram, 2007; Alexander et al., 2005, 2008), synchronous period doubling in the flicker ERG occurred within a relatively narrow range of stimulus temporal frequency. The stimulus frequency region over which the phenomenon was observed (approximately 32 Hz to 62 Hz) was highly similar for the control subjects and the two diabetic groups. The abrupt emergence (and disappearance) of period doubling with small changes in stimulus temporal frequency was first shown by Crevier and Meister (1998) in the salamander retina. They reported that the phenomenon develops suddenly, within a fraction of 1 Hz. This narrow tuning can be appreciated in Fig. 1, where period doubling is absent in the waveform of Subject 2 at 33.3 Hz and clearly present at 35.7 Hz. Individual diabetic subjects also showed narrow frequency tuning and the frequency range over which period doubling occurred did not differ from the controls. As a group, however, the amplitude of the 3F/2 and 5F/2 components were reduced significantly in the mild NPDR subjects.

The finding that period doubling in the diabetic retina occurs over the same frequency range as that of the controls, but the magnitude of the phenomenon is reduced, can be explained within the context of Crevier and Meister's non-linear feedback model. Specifically, the diabetic data can be best accounted for by a reduction in the magnitude of the feedback signal, rather than a change in the feedback decay time. The specific mechanism responsible for the reduced feedback in mild NPDR subjects is presently uncertain. However, it is likely that the site of the abnormality is post-receptor, based on a pharmacological dissection of the salamander retina. Crevier and Meister (1998) showed that the isolated salamander photoreceptor response does not exhibit period doubling, indicating that nonlinearities in phototransduction do not generate the phenomenon. Likewise, blocking amacrine and retinal ganglion cell function did not affect period doubling, indicating that inner-retina circuitry is not essential for the phenomenon to occur. Crevier and Meister (1998) blocked depolarizing bipolar cell pathway function using APB and showed that period doubling persisted, despite the absence of ON responses. On the other hand, period doubling was eliminated by blocking hyperpolarizing bipolar cell pathway function (using kynurenic acid or CNQX + AP7), indicating an essential role for the OFF bipolar cell pathway. Thus, the minimum circuit needed to generate period doubling, at least in the salamander retina, consists of cone photoreceptors and OFF bipolar cells. Extrapolating these findings, the reduced (or absent) period doubling in mild NPDR subjects may result from abnormalities in signal transmission from the cone

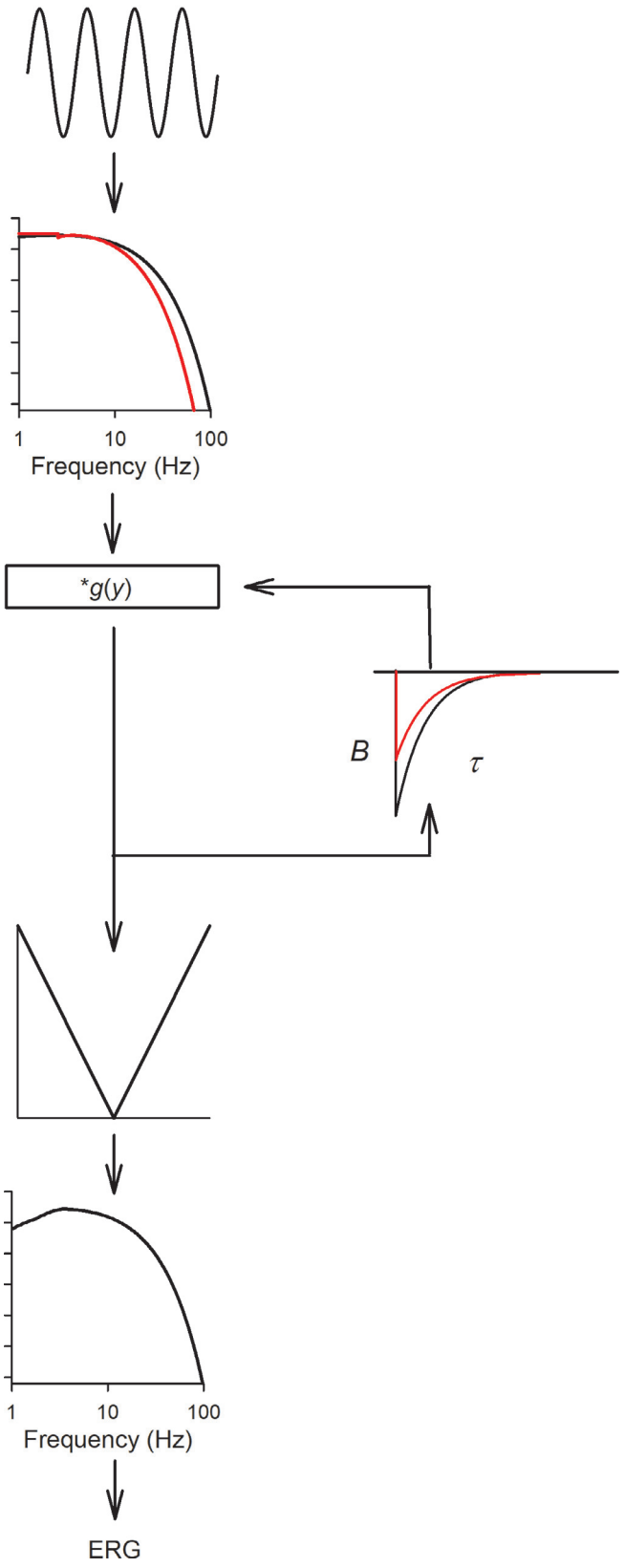

Fig. 7. Schematic illustration of the expanded sandwich model. The illustration is derived from Alexander et al. (2005) and Crevier and Meister (1998), as described in the text.

photoreceptors to OFF bipolar cells, or from abnormalities in the OFF bipolar cell itself. However, more work is needed to evaluate this speculation.

As discussed above, flicker ERG abnormalities in NPDR have been described within the context of a linear-nonlinear-linear cascade ("sandwich") model of retinal processing (McAnany & Park, 2018b). The putative non-linear feedback circuit that underlies period doubling can be included in an expanded sandwich model (Alexander et al., 2005), which helps to further insight into the sites and mechanisms of retinal dysfunction in NPDR. Specifically, according to the sandwich model of the ERG (schematized in Fig. 7), there is an early low-pass linear filter that is presumed to be localized to the photoreceptors (Burns et al., 1992). The low-pass filter is followed by a nonlinearity (e.g. rectifier) that generates the harmonic components of the flicker ERG. The nonlinearity is thought to be localized prior to (or at) the cone-bipolar cell synapse where different spectral classes of cones converge (Chang, Burns, & Kreitz, 1993; Lee, Dacey, Smith, & Pokorny, 1999). The nonlinearity, in turn, is followed by a second linear filter that has bandpass characteristics, consistent with the bandpass temporal filtering of bipolar cells (Kondo & Sieving, 2001). Previous work has argued that high frequency flicker ERG abnormalities can likely be attributed to a shift in the high frequency cutoff of the initial linear low-pass filter (McAnany & Park, 2018b). An abnormality in the initial linear filter could reduce the fundamental amplitude of the high frequency flicker ERG without affecting the high frequency harmonics that are elicited by slow flicker. Thus, in Fig. 7, the initial low-pass filter is shifted to the left in the diabetic model (red) compared to the control (black). The other stages of filtering are presumed to be unaffected by diabetes. As noted above, the nonlinear feedback that generates period doubling is likely located at the synapse between the photoreceptors and bipolar cells (Crevier & Meister, 1998). As such, previous work has positioned the feedback mechanism between the initial low-pass filter and the nonlinearity (Alexander et al., 2005). This results in the output of the initial linear filter being multiplied by the variable gain that depends on the feedback signal, as shown in Fig. 7. The subharmonic (F/2) is then passed through the nonlinearity, which generates harmonics of the subharmonic (3F/2, 5F/2). Finally, these are passed through the bandpass filter, which attenuates the F/2 response to near noise levels (see Fig. 2). For the mild NPDR subject group, the magnitude of the feedback signal may be decreased (indicated by the red exponential function), relative to the control subjects (black exponential function). Thus, in this expanded sandwich model, the diabetics' reduction in signal feedback is presumed to be independent of the photoreceptor abnormality that affects the high-frequency cutoff of the initial linear low-pass filter.

In conclusion, the flicker ERG of visually-normal individuals can show synchronous period doubling over a narrow band of stimulus temporal frequencies. The flicker ERG of diabetic subjects can also show synchronous period doubling, but the magnitude of the phenomenon is reduced, on average, and is completely absent in some patients. Analysis of harmonic and subharmonic responses elicited by sinusoidal stimuli that span a range of temporal frequencies can be useful for understanding the sites and mechanisms that underlie retinal dysfunction in diabetes and other retinal diseases. The approach presented here may be useful for generating hypotheses regarding the sites and mechanisms of disease that can be evaluated in animal models. Although the approach to evaluate the harmonic and subharmonic components of the flicker ERG was described in the context of diabetic retinopathy, we anticipate that this type of analysis may be of use in other retinal disorders as well.

Acknowledgments

This research was supported by National Institutes of Health research grants R01EY026004 (JM), P30EY001792 (core grant), UL1TR000050 (Center for Clinical and Translational Science), an

unrestricted departmental grant and a Dolly Green Scholar award (JM) from Research to Prevent Blindness.

References

Alexander, K. R., Barnes, C. S., & Fishman, G. A. (2001). Origin of deficits in the flicker electroretinogram of the cone system in X-linked retinoschisis as derived from response nonlinearities. *Journal of the Optical Society of America. A, Optics, Image Science, and Vision, 18*(4), 747–754.

Alexander, K. R., Fishman, G. A., & Grover, S. (2000). Temporal frequency deficits in the electroretinogram of the cone system in X-linked retinoschisis. *Vision Research, 40*(20), 2861–2868.

Alexander, K. R., Levine, M. W., & Super, B. J. (2005). Characteristics of period doubling in the human cone flicker electroretinogram. *Visual Neuroscience, 22*(6), 817–824.

Alexander, K. R., & Raghuram, A. (2007). Effect of contrast on the frequency response of synchronous period doubling. *Vision Research, 47*(4), 555–563.

Alexander, K. R., Raghuram, A., & McAnany, J. J. (2008). Comparison of spectral measures of period doubling in the cone flicker electroretinogram. *Documenta Ophthalmologica, 117*(3), 197–203.

Baker, C. L., Jr., & Hess, R. F. (1984). Linear and nonlinear components of human electroretinogram. *Journal of Neurophysiology, 51*(5), 952–967.

Burns, S. A., Elsner, A. E., & Kreitz, M. R. (1992). Analysis of nonlinearities in the flicker ERG. *Optometry and Vision Science, 69*(2), 95–105.

Chang, Y., Burns, S. A., & Kreitz, M. R. (1993). Red-green flicker photometry and nonlinearities in the flicker electroretinogram. *Journal of the Optical Society of America A: Optics, Image Science, and Vision, 10*(6), 1413–1422.

Crevier, D. W., & Meister, M. (1998). Synchronous period-doubling in flicker vision of salamander and man. *Journal of Neurophysiology, 79*(4), 1869–1878.

Davis, M. D., Fisher, M. R., Gangnon, R. E., Barton, F., Aiello, L. M., Chew, E. Y., et al. (1998). Risk factors for high-risk proliferative diabetic retinopathy and severe visual loss: Early Treatment Diabetic Retinopathy Study Report #18. *Investigative Ophthalmology & Visual Science, 39*(2), 233–252.

Geraci, M. (2014). Linear quantile mixed models: The lqmm package for LAPLACE quantile regression. *Journal of Statistical Software, 57*(13), 1–29.

Geraci, M., & Bottai, M. (2007). Quantile regression for longitudinal data using the asymmetric Laplace distribution. *Biostatistics, 8*(1), 140–154.

Geraci, M., & Bottai, M. (2014). Linear quantile mixed models. *Statistics and Computing, 24*(3), 461–479.

Gouras, P., & Gunkel, R. D. (1962). The resonant frequencies of rod and cone electroretinograms. *Investigative Ophthalmology and Visual Sciences, 1*(1), 122–126.

Gouras, P., & Gunkel, R. D. (1964). The frequency response of normal, rod achromat and nyctalope ergs to sinusoidal monochromatic light stimulation. *Documenta Ophthalmologica, 18*, 137–150.

Hassan-Karimi, H., Jafarzadehpur, E., Blouri, B., Hashemi, H., Sadeghi, A. Z., & Mirzajani, A. (2012). Frequency domain electroretinography in retinitis pigmentosa versus normal eyes. *Journal of Ophthalmic & Vision Research, 7*(1), 34–38.

Kondo, M., & Sieving, P. A. (2001). Primate photopic sine-wave flicker ERG: Vector modeling analysis of component origins using glutamate analogs. *Investigative Ophthalmology & Visual Science, 42*(1), 305–312.

Lee, B. B., Dacey, D. M., Smith, V. C., & Pokorny, J. (1999). Horizontal cells reveal cone type-specific adaptation in primate retina. *Proceedings of the National Academy of Sciences of the United States of America, 96*(25), 14611–14616.

McAnany, J. J., & Nolan, P. R. (2014). Changes in the harmonic components of the flicker electroretinogram during light adaptation. *Documenta Ophthalmologica, 129*(1), 1–8.

McAnany, J. J., & Park, J. C. (2018a). Amplitude loss of the high-frequency flicker electroretinogram in early diabetic retinopathy. *Retina* in press.

McAnany, J. J., & Park, J. C. (2018b). Temporal frequency abnormalities in early-stage diabetic retinopathy assessed by electroretinography. *Investigative Ophthalmology and Visual Sciences, 59*(12), 4871–4879.

McAnany, J. J., & Park, J. C. (2019). Cone photoreceptor dysfunction in early-stage diabetic retinopathy: Association between the activation phase of cone phototransduction and the flicker electroretinogram. *Investigative Ophthalmology and Visual Sciences, 60*(1).

McCulloch, D. L., Marmor, M. F., Brigell, M. G., Hamilton, R., Holder, G. E., Tzekov, R., et al. (2015). ISCEV standard for full-field clinical electroretinography (2015 update). *Documenta Ophthalmologica, 130*(1), 1–12.

Odom, J. V., Reits, D., Burgers, N., & Riemslag, F. C. (1992). Flicker electroretinograms: A systems analytic approach. *Optometry and Vision Science, 69*(2), 106–116.

Park, J. C., Cao, D., Collison, F. T., Fishman, G. A., & McAnany, J. J. (2015). Rod and cone contributions to the dark-adapted 15-Hz flicker electroretinogram. *Documenta Ophthalmologica, 130*(2), 111–119.

Porciatti, V., & Falsini, B. (1993). Inner retina contribution to the flicker electroretinogram: A comparison with the pattern electroretinogram. *Clinical Vision Science, 8*, 435–447.

Sieving, P. A., Arnold, E. B., Jamison, J., Liepa, A., & Coats, C. (1998). Submicrovolt flicker electroretinogram: Cycle-by-cycle recording of multiple harmonics with statistical estimation of measurement uncertainty. *Investigative Ophthalmology & Visual Science, 39*(8), 1462–1469.

Spekreijse, H., & Reits, D. (1982). Sequential analysis of the visual evoked potential system in man: Nonlinear analysis of a sandwich system. *Annals of the New York Academy of Sciences, 388*, 72–97.

Viswanathan, S., Frishman, L. J., & Robson, J. G. (2002). Inner-retinal contributions to the photopic sinusoidal flicker electroretinogram of macaques. Macaque photopic sinusoidal flicker ERG. *Documenta Ophthalmologica, 105*(2), 223–242.